



## Mineralogical and geochemical investigations of sediment-source region changes in the Okinawa Trough during the past 100 ka (IMAGES core MD012404)

Huei-Fen Chen<sup>a,\*</sup>, Yuan-Pin Chang<sup>b</sup>, Shuh-Ji Kao<sup>c</sup>, Min-Te Chen<sup>a</sup>, Sheng-Rong Song<sup>d</sup>, Li-Wei Kuo<sup>d</sup>, Shie-Ying Wen<sup>a</sup>, Tien-Nan Yang<sup>e</sup>, Teh-Quei Lee<sup>e</sup>

<sup>a</sup> Institute of Applied Geosciences, National Taiwan Ocean University, Keelung 20224, Taiwan

<sup>b</sup> Institute of Marine Geology and Chemistry, National Sun Yat-Sen University, Kaohsiung 80424, Taiwan

<sup>c</sup> Research Center for Environmental Changes, Academia Sinica, Taipei 11529, Taiwan

<sup>d</sup> Institute of Geosciences, National Taiwan University, Taipei 10617, Taiwan

<sup>e</sup> Institute of Earth Sciences, Academia Sinica, Taipei 11529, Taiwan

### ARTICLE INFO

#### Article history:

Available online 3 November 2010

#### Keywords:

Okinawa Trough  
Kuroshio Current  
Yangtze River  
Asian monsoon  
Sediment

### ABSTRACT

We present a mineralogical and geochemical study of core MD012404, retrieved from the central Okinawa Trough (OT) of the East China Sea. Our studies reveal that the sediment sources of the core have been changed through time during the past 100 ka. Our mineralogical proxies indicate that the sediments source from the Yangtze River correlates well sea-level changes before 24 ka. Our Ti/Al ratios otherwise indicate an increase of sediment supply from eastern Taiwan after 26 ka. The cooler climate of the Last Glacial Maximum (LGM, 23~19 ka) led to a reduction in fluvial sediments from the Yangtze River. However, subsequent climate warming (after ~19 ka) resulted in an abrupt increase in fluvial sediments. After the LGM, the Kuroshio intrusion flow into the OT may have increased. We also infer anomalous changes in eolian sources transported by winter monsoons during the LGM and at 80 ka based on an eolian mineralogical indicator (feldspar). We conclude that the sediment source of core MD012404 is primarily of terrestrial origins, but influenced by sea-level changes and variations in the East Asian monsoon.

© 2010 Elsevier Ltd. All rights reserved.

### 1. Introduction

Core MD012404 (26°38.84'N, 125°48.75'E; water depth 1397 m) was retrieved from the central Okinawa Trough (OT) in the IMAGES (International Marine Past Global Change) cruise with an aim of studying sediment source changes in the OT (Bassinot et al., 2002; Chang et al., 2005, 2008, 2009; Kao et al., 2006). The coring site is close to the southern end of the East China Sea (ECS) at the western edge of the Pacific Ocean (Fig. 1); its sediments are mostly derived from flux along ECS continental shelves and the Kuroshio Current (KC). Fortunately, core MD012404 offers high sampling resolution and covers a long depositional history (~100 ka), thereby, affording the relationship between sedimentary sources and sea-level changes on a glacial–interglacial time-scale, and allowing us to judge variation in the influence of the Asian monsoon associated with climate change in the study area.

The ECS is a large marginal sea along the east coast of the Asian continent, stretching from 24°N to 32°N. Most sedimentary deposits along ECS shelves are derived from the Yangtze River (Fig. 1).

\* Corresponding author. Address: 2 Pei-Ning Road, Keelung 20224, Taiwan, ROC. Tel.: +886 2 24622192x6519; fax: +886 2 24625038.

E-mail address: [diopside0412@yahoo.com.tw](mailto:diopside0412@yahoo.com.tw) (H.-F. Chen).

Previous studies have shown that sediments deposited in the Yangtze Estuary arrive carried on an annual fresh water discharge that is as high as  $9 \times 10^{11} \text{ m}^3$  (Chen et al., 1988, 2001). At present, sediments deposited near the Yangtze Estuary are carried southward by the China Coastal Current (CCC) in winter while sediments deposited away from the estuary (offshore) are carried northward by the Taiwan Warm Current (TWC) in summer (Beardsley et al., 1985; Lee and Chao, 2003). Such transport leads to an extensive alongshore mud wedge, extending to the Taiwan Strait. Liu et al. (2006) proposed southward transport of Yangtze-derived sediment during the last 7 ka caused by the newly formed CCC after high-stand sea-levels were reached in the mid-Holocene. The southward elongation of this shore-parallel mud wedge is facilitated by the downwelling CCC and upwelling TWC, which also helps to block the escape of Yangtze River sediment to the OT. The first question we wish to resolve with this research is whether Yangtze-derived sediment reached the mid-OT more readily between 7 ka and 100 ka, especially in the Last Glacial Maximum (LGM) when sea-levels were at their lowest. In which case, detrital sediments from the Yangtze River are our first concern.

The second issue is the dynamic development of the KC. This is the main ocean current flowing into the OT. It flows northward along the east coast of Taiwan, and then eastward to the OT (Liu et al.,

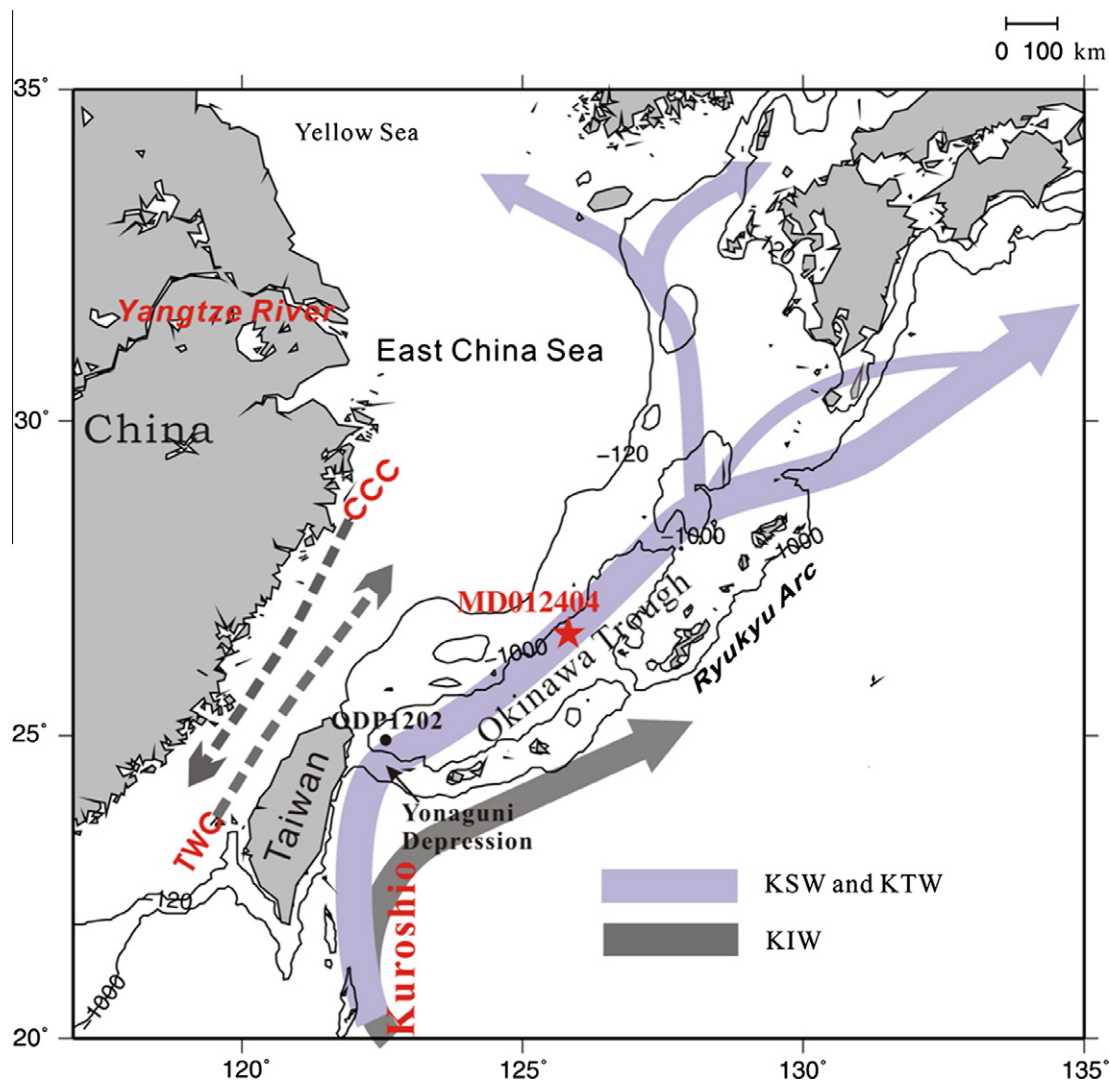


**Fig. 1.** Map showing the location and regional topography of core MD012404 (star mark) in the central Okinawa Trough (OT) at the southern of the East China Sea (ECS). The Kuroshio is divided into the Kuroshio Surface Water (KSW), Kuroshio Tropic Water (KTW), and Kuroshio Intermediate Water (KIW) dependent on depths as per Chen et al. (1995a). The upper KSW and KIW flow into the OT, but most of the KIW is blocked by the Ryukyu Ridge, and a lower breach of the Yonaguni Depression in the southwestern part of the ridge is at a water depth of about 300–600 m (Chang et al., 2009). Another core, ODP1202 (circle mark), is located in the southern part of the OT near eastern Taiwan. The Chinese Coastal Current (CCC) flows southwardly offshore of the ECS in winter, and the Taiwan Warm Current (TWC) enters northwardly from the Taiwan Strait in summer (Beardsley et al., 1985; Lee and Chao, 2003).

1999) (Fig. 1). Core ODP1202 that was drilled from the southernmost part of the OT which is close to the northern foot of the I-Lan Ridge, providing a 410-m long sediment section covering the last 127 ka of the late Quaternary (Wei et al., 2005). The upper 110 m of the core is mainly composed of fine-grained clay and silty clay sediments. Below 110 m (~28 ka) of the core, however, the sediments are composed of turbidites with slate fragments, and metamorphic and volcanic debris (Huang et al., 2005). Diekmann et al. (2008) studied sediment source variations in the southern OT using core ODP1202. Unfortunately, however, their time scale is too short to show relations between cycles in sea-level changes over the past 100 ka. Although this coring site is not as sensitive as site MD012404, which is closer to the Yangtze River (Fig. 1), ODP1202 provides useful reference data relevant to the tectonic history of the OT. Huang et al. (2005) reported that a series of mass-wasting events are recorded in ODP 1202, which might have been triggered by tectonic events in the southern OT. In this study, we adopted mineralogical and geochemical approaches to study the sediment source variations of core MD012404, with a high quality age control

of the core (Chang et al., 2005, 2008; Kao et al., 2006). Our studies provide better constraints on the timing of the shifting of sediment input into the OT within a context of climate changes expressed by sea level, KC, and the East Asian monsoon.

## 2. Regional setting and the Kuroshio Current

The coring site of core MD012404 is situated on the continental slope of the ECS in the central OT (Fig. 1). The OT is a backarc-spreading basin that extends in a northeast–southwest direction between the ECS shelf and the Ryukyu arc. Coring Site MD012404 is located about equal distance from the Yangtze Estuary and eastern Taiwan. Presently, the ECS receives its sediments mostly from the Yangtze River (Liu et al., 2006), which originates in the Qinghai–Tibetan Plateau at an elevation of 6600 m, then it flows eastward for more than 6300 km. It is the largest river in Asia and is the third longest river in the world (Milliman and Meade, 1983). The Yangtze River contributes enormous fresh water and nutrients into the ECS.

On the other hand, the KC originates from the westward flowing North Equatorial Current in the central Pacific, and flows into the southern edge of the OT (Fig. 1). The KC is an important carrier of heat and moisture from the western Pacific warm pool to the middle latitudes of the northern Pacific Ocean (Hsin et al., 2008; Andres et al., 2008). The Kuroshio axis is located over the upper continental slope of the ESC, shifting laterally in the flow path through the seasons (Andres et al., 2008). However, the KC might have migrated to the east of the Ryukyu Islands rather than flowing into the OT during the LGM due to lower sea-levels under the emergence of a Ryukyu–Taiwan Ridge (Ujiié et al., 1991, 2003; Kao et al., 2006; Chang et al., 2008; Diekmann et al., 2008). Intensified KC inflow at the beginning of the Holocene introduced abundant warm-species fauna into the OT (Jian et al., 2000; Ujiié et al., 2003; Ijiri et al., 2005), and Japan Sea (Oba, 1990).

In addition, the KC has shallow, mid-level, and deep water systems, and brings saline water to the OT (Chen et al., 1995b; Nakamura et al., 2008). The shallow KC is named Kuroshio Surface Water (KSW). KSW comprises the upper 100 m of the KC and is nutrient depleted. The mid-level KC is named Kuroshio Tropic Water (KTW); it has the highest salinity of all KC water and is situated between a depth of 100 and 300 m. The deep KC, named Kuroshio Intermediate Water (KIW), is centered at a depth of 600 m; it exhibits minimum salinity and the highest nutrient content of all KC water (Chen et al., 1995a,b). As mentioned, maximum salinity exists in the KTW, and nutrient content increases gradually with depth to reach maximum concentration in the KIW zone. Chen (1996) considered KIW to be the major source of nutrients on the ECS continental shelf. However, Chen and Wang (1998) suggested that KIW is largely blocked by the ridge along eastern Taiwan, forcing KIW to turn eastward. The ridge divides the KIW into two parts. The upper part is Intermediated Water of the South China Sea (i.e., that above a depth of 500 m) coming from the KC's southwestern edge, while the deeper KIW is Pacific Intermediate Water coming from the North Equatorial Current in the central Pacific. In this paper, we accept the latter research of Chen and Wang (1998), and determine the current model given in Fig. 1. Only upper KIW can enter the OT, whilst most of KIW turns eastward after being blocked by the Ryukyu Ridge.

### 3. Detrital Sediment Sources

Presently, coring site MD012404, near the central OT, is far from its two main sedimentary-sources of eastern Taiwan and the Yangtze River Estuary (Fig. 1). The former source is mainly derived from the KC's northeastward flow and the latter by the flow of the TWC; transportation over such long distances means that carried sediments are generally very fine and homogeneous. In fact, core sediments of MD012404 are generally finer than those of core ODP1202 (mud, silt, and sand layers), extracted near eastern Taiwan. Sediments of core MD012404 are mainly composed of nearly homogenous silty mud and pure mud. No visible turbidites or tephra layers were found in the core, but pumice and volcanic glass can be observed under the microscope at some depths (Bassinot et al., 2002; Chang et al., 2008).

Most modern Yangtze River discharge occurs in summer. Between June and September, river accumulations near the river mouth amount to about 4.4 cm. In contrast, annual accumulation rates are about 1–6 cm/year (McKee et al., 1983; DeMaster et al., 1985; Chen et al., 2004; Liu et al., 2006). Suspended sediments of the Yangtze River are derived from both the Tibetan Plateau and the low lands of Eastern China (Yang et al., 2003, 2004). Quartz and feldspar are dominant minerals with average total contents of about 71% in Yangtze River sediments (Yang et al., 2004). In clay fractions, illite and chlorite are the major clay minerals, and minor

fractions of kaolinite and smectite can be found in deposits along the ECS. These are at levels slightly higher than those of the north-western Taiwan shelves (Chen, 1973; Aoki and Oinuma, 1974; Lin and Chen, 1983; Eisma et al., 1995).

Diekmann et al. (2008) found that the detrital minerals in ODP1202 were primarily derived from Taiwan, which are characterized by higher compositions of illite and chlorite but lesser amounts of kaolinite and smectite (Aoki and Oinuma, 1974; Chen, 1973; Lin and Chen, 1983). In Taiwan, illite and chlorite are abundant in the widespread slates and greenschists of eastern Taiwan; they are also evident in soils and Neogene to Pleistocene deposits, whereas kaolinite and smectites are much less abundant (Chen, 1973; Dorsey et al., 1988). In central Taiwan, slate is dominant in the Lushan Formation of the Central Mountain Range; slate sediments are carried by the Lan-Yang River and distributed along the northeastern Taiwan shelf. In eastern Taiwan, widespread greenschists are readily eroded by eastward flowing rivers and deposited along eastern Taiwan shelves. These deposits are picked up and transported by the TWC and KC to the OT (Fig. 1).

In the above research descriptions, researches only concentrated on clay fractions (<2 µm), comparing the amounts of different clays, but ignoring the contributions of quartz and feldspar in bulk sediments. However, it is possible to estimate changes in detrital sources by comparing sedimentation rates and variations in mineral assemblages even when transport distances and environmental energy affect grain size distributions and the percentage of quartz and feldspar in bulk sediments. For example, feldspar can

**Table 1**

Age control points used to derive age model of core MD012404 (Chang et al., 2009). Nineteen AMS <sup>14</sup>C dated points were calibrated by using Fairbanks et al.'s (2005) function. Remained seven points were graphic correlation based upon Martinson's dataset that tuned by orbital forcing. MIS = Marine Isotope Stage.

Depth (cm)	AMS <sup>14</sup> C age ± error <sup>a</sup>	Calendar age (year)	Species
14.5	1040 ± 70	769	<i>G. sacculifer</i>
104.5	2350 ± 30	2193	<i>G. sacculifer</i> + <i>G. ruber</i>
254.5	4500 ± 110	4891	<i>G. sacculifer</i>
349.5	6450 ± 30	7202	<i>G. sacculifer</i> + <i>G. ruber</i>
494.5	9730 ± 120	10,863	<i>G. sacculifer</i>
589.5	10,820 ± 190	12,585	<i>G. sacculifer</i>
624.5	11,370 ± 40	13,112	<i>G. sacculifer</i> + <i>G. ruber</i>
744.5	12,680 ± 130	14,620	<i>G. sacculifer</i>
854.5	13,950 ± 90	16,514	<i>G. sacculifer</i>
904.5	14,560 ± 45	17,407	<i>G. sacculifer</i> + <i>G. ruber</i>
1019.5	15,810 ± 160	18,843	<i>G. sacculifer</i>
1194.5	19,520 ± 230	23,057	<i>G. sacculifer</i>
1379.5	21,360 ± 70	25,382	<i>G. sacculifer</i> + <i>G. ruber</i>
1454.5	23,230 ± 270	27,561	<i>G. sacculifer</i>
1539.5	24,450 ± 490	28,912	<i>G. sacculifer</i>
1719.5	27,970 ± 200	32,554	<i>G. sacculifer</i> + <i>G. ruber</i>
1914.5	30,200 ± 230	35,051	<i>G. sacculifer</i> + <i>G. ruber</i>
2074.5	32,490 ± 1110	37,252	<i>G. sacculifer</i> + <i>G. ruber</i>
2174.5	34,010 ± 280	38,830	<i>G. sacculifer</i> + <i>G. ruber</i>
2429.5		43,880	MIS 3.13
2809.5		50,210	MIS 3.3
3004.5		55,450	MIS 3.31
3139.5		64,090	MIS 4.22
3474.5		70,820	MIS 4.24
3824.5		79,250	MIS 5.1
4094.5		90,950	MIS 5.2

<sup>a</sup> Error is gave in 1σ.

be used as a marker of aeolian sources. The proportion of feldspar to quartz reflects aeolian sources in relation to China and Taiwan as feldspar ratios are high in north China but very low in Taiwan (Table 2). Evidence of this is given in Section 6 and normalized mineral assemblages are shown in Fig. 4. In Eastern China, granite is the main protolith leading to erosion sediments being rich in quartz and feldspar. On the other hand, in eastern Taiwan, metamorphic rocks are rich in illite, muscovite, and chlorite. This difference in major mineral assemblages can be used to estimate the origins of sediments. (Note: the amounts of minor clay minerals of kaolinite and smectite are so small that they are often below the calibrated analysis error of the X-ray Powder Diffraction (XRD) method used.) Geochemical properties are also useful in this examination as Ti/Al ratios differ distinctly between continental and oceanic crusts (Table 3). Consequently, we can use this distinction to identify sediments from eastern Taiwan, where the Coastal Range is partially composed of oceanic crust.

To summarize, terrestrial-sediment sources at coring site MD012404 are: (1) re-deposited sediments from the ECS; (2) weathered slates from the Lan-Yang River and weathered greenschists from eastern Taiwan carried by the KC and TWC; and (3) aeolian sources from northern China. Contributions from Source (1) are potentially controlled by transportation distance from the Yangtze Estuary; and these sediments are characterized by quartz and feldspar with minor illite and chlorite. Source (2) is composed of illite and chlorite predominantly, and possesses higher Ti/Al ratios. Source (3) can be referenced by the proportion of feldspar to quartz in marine sediments.

#### 4. Methods

Semi-quantitative analysis of major minerals is provided by XRD (MAC Science, model MXP 3) while conventional X-ray Fluorescence (XRF) is used for the chemical quantification of major elements. Samples were taken at 5-cm intervals for sediments deposited after 20 ka, representing an average sample resolution of about 0.1 ky, and at 10–20 cm for sediments deposited before 20 ka. As mentioned, many previous studies used only the clay fraction to probe sediment sources and mostly ignored major min-

**Table 3**

Comparison between our data and Ti/Al ratio data referenced from previous reports (world averages).

	TiO <sub>2</sub>	Al <sub>2</sub> O <sub>3</sub>	100Ti/ Al	References
Upper continental crust	0.64	15.40	2.65	Rudnick and Gao (2003)
Middle continental crust	0.69	15.00	2.93	
Lower continental crust	0.82	16.90	3.09	
Total continental crust	0.72	15.90	2.89	
Upper continental crust	0.5	15.20	2.10	Rudnick and Fountain (1995)
Middle continental crust	0.7	15.50	2.88	
Lower continental crust	0.8	16.60	3.07	
Total continental crust	0.7	15.80	2.82	
Felsic rocks	0.48	14.00	2.19	Rudnick and Fountain (1995)
Intermediate rocks	0.97	16.80	3.68	
Mafic rocks	1.32	15.80	5.33	
0–26 ka	0.78	16.90	2.93	This study of MD012404
26–100 ka	0.76	17.53	2.76	

erals such as quartz and feldspar. We take into account the most important source of quartz, mainly the Yangtze River in southern China. Bulk sediments are used to analyze major mineral components and bio-source carbonate content. Ready comparison can be made between our semi-quantitative method for calcite and traditional acid treatment results (see Chang et al. (2005) for acid treatment method and results), allowing for carbonate content to be used in confirming the validity of the semi-quantification method (Fig. 2).

Semi-quantification of major minerals by XRD used a Cu target under conditions: 45 kV and 40 mA, divergence slit 0.5°, scanning step size 0.0083556°/s, and per time step of 1.27 s in a 2θ range between 3° and 80°. All major minerals are identified.

**Table 2**

Major mineral contents in China and Taiwan from high latitude to low latitude regions, including the regional sources of aeolian dust in Inner Mongolia and Nihawan Basin near the Loess Plateau. The data from Yellow River and Yangtze River are quoted from Yang et al. (2004), who quantified major minerals by microscope and clay fractions by XRD. All the data from Taiwan are from cored lake sediments (unpublished data).

Locality	Longitude and latitude	Illite and muscovite	Chlorite and kaolinite	Quartz	Feldspar	Calcite and dolomite	F/(F + Q) <sup>a</sup>	Annotation
Inner Mongolia in north China (Eastern Juyanhai <sup>c</sup> )	42°20.13'N 101°15.35'E	1.28	1.67	64.93	25.28	6.48	0.28	Chen et al. (2010)
		5.71	6.65	45.73	10.24	27.19	0.18	
Hebei Province in north China (Nihawan Basin)	40°03.988'N 114°06.24'E	7.5	9.4	53.7	16.6	12.8	0.24	Averaged result of upper 500 cm in a core <sup>b</sup>
Yellow River in north China (North China)	32°10'–41°50'N 95°53'–119°05'E	13.5	3.5	41	34a	6.8	0.45	Yang et al. (2004) samples near middle and lower reaches in channel and floodplains
Yangtze River in south China (South China)	24°27'–35°44'N 90°33'–122°19'E	15.0	6.1	42	29	6.8	0.41	Yang et al. (2004) samples near the lower reaches in channel and floodplains
Northeastern Taiwan (Meiha Lake)	24°38.537'N 121°43.952'E	31.3	30.5	33.0	5.2	0	0.036	Averaged result of upper 700 cm in a core <sup>b</sup>
Central Taiwan (Liyutan Lake)	23°57.833'N 120°59.417'E	17.5	17.2	62.1	2.5	0	0.04	Average result of upper 1000 cm in a core <sup>b</sup>
South Taiwan (Tung-Yuan Pond)	22°12.341'N 120°51.312'E	17.6	11.2	68.1	3.2	0	0.04	Average result of upper 1500 cm in a core <sup>b</sup>

<sup>a</sup> F/(F + Q) = feldspar/(feldspar + quartz).

<sup>b</sup> Our unpublished data.

<sup>c</sup> The first row is the averaged result of the upper 112 cm in a core (lakeshore and aeolian sand); the second row is the averaged result between 112 and 406 cm (lacustrine mud and silty mud) in a core.

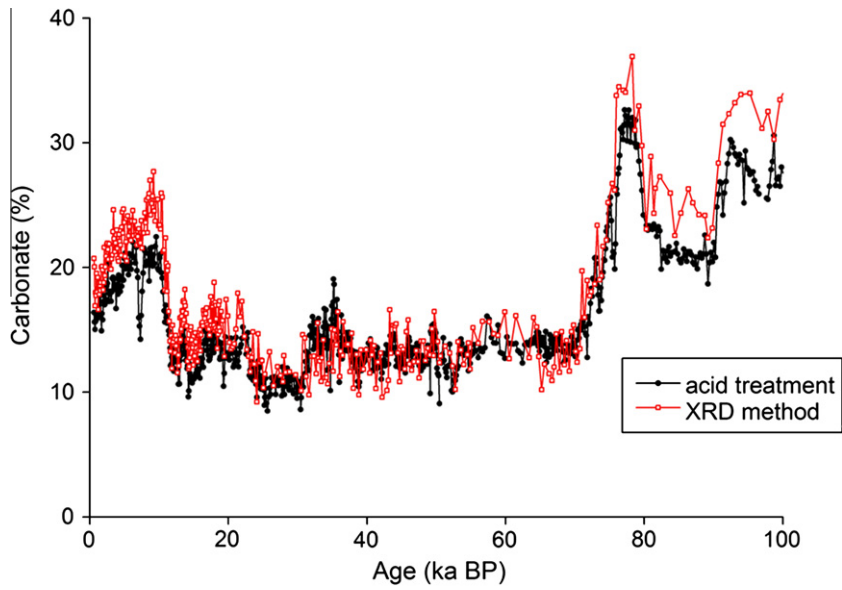


Fig. 2. Comparisons of the carbonate contents of the acid treatment method with XRD method in this study. Results indicate a very good relation between them, especially when the percentage is under 25%.

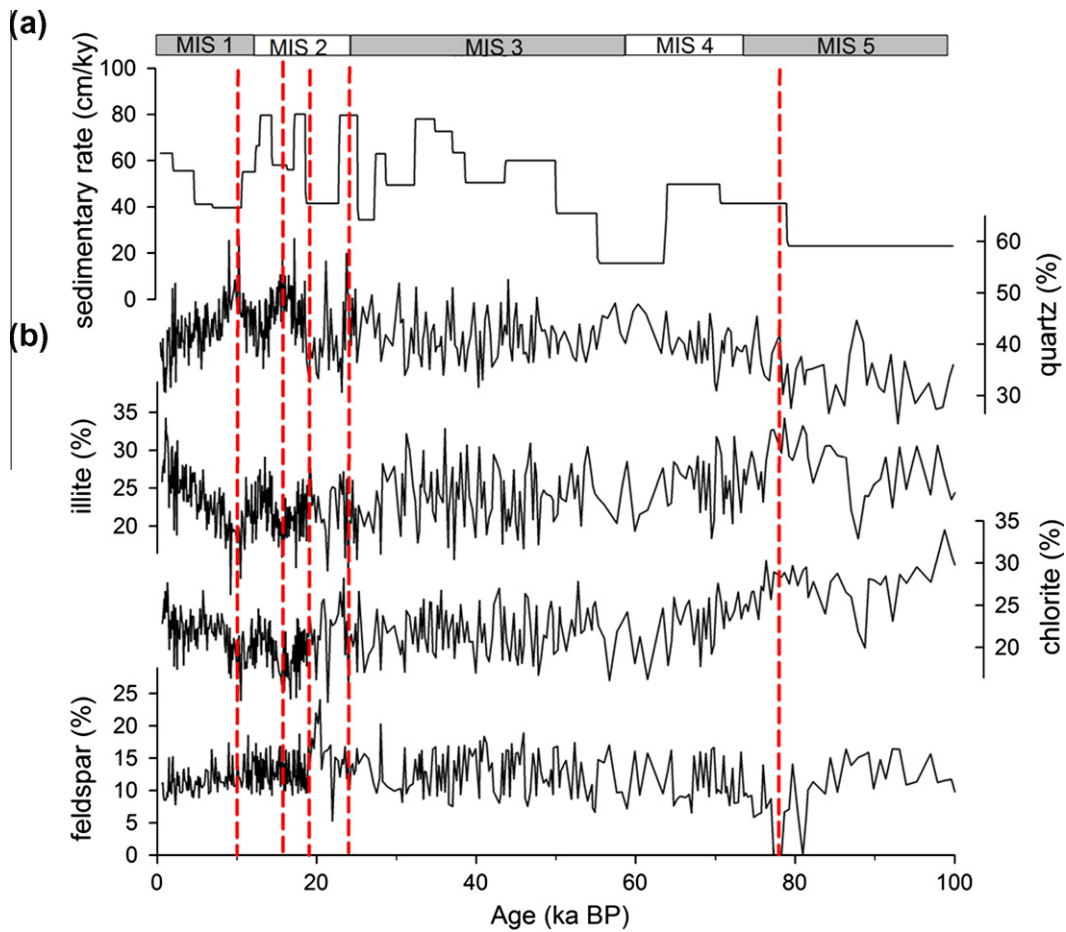
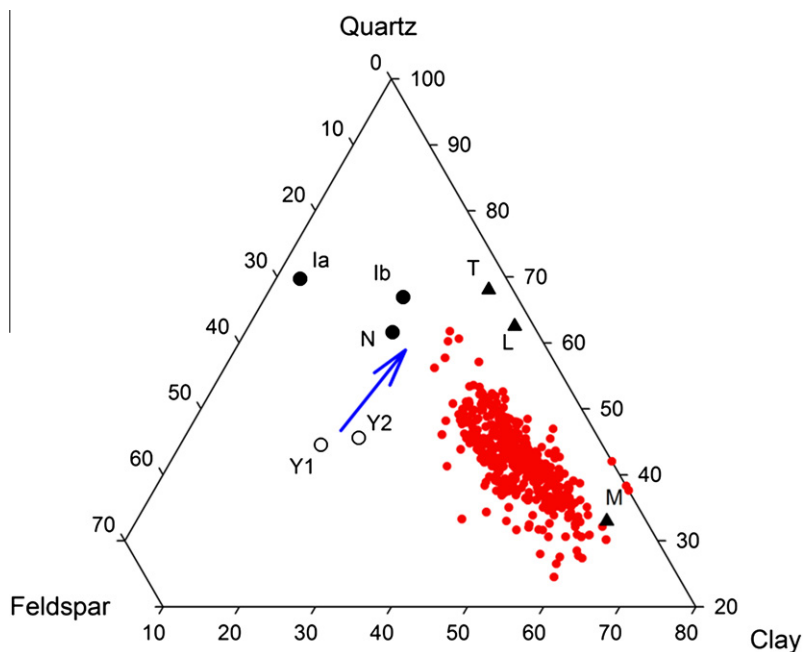


Fig. 3. (a) Sedimentation rates, and (b) major mineral variations of core MD012404 during the past 100 ka. The calculation of sedimentation rates is based on the age model of Table 1. The relative percentages of the detrital minerals include: quartz, illite, chlorite, and minor feldspar. After 20 ka, the data points had higher resolution. The dashed-red lines represent the time boundaries at: 78.3 ka, 24 ka, 19 ka, 16 ka, and 10 ka. (For interpretation of the references to colour in this figure legend, the reader is referred to the web version of this article.)



**Fig. 4.** A ternary plot using quartz, feldspar and clay minerals as the end components shows the normalized mineral percentages from the data in Table 2. la: aeolian and lakeshore sand in Eastern Juyanhai; lb: lake mud in Eastern Juyanhai; N: Nihawan Basin; L: Liyutan Lake; T: Tung-Yuan Pond; M: Meiha Lake in our unpublished data; Y1: Yellow River; and Y2: Yangtze River (determined from Yang et al. (2004)). Y1 and Y2 are derived from microscopy of coarse grains and likely have more feldspar than our data. Y1 includes deposited sediments from the Löss Plateau, and its lithology is very similar to our Nihawan Basin (N); consequently, Y1 and Y2 should be reflected in the trend of our analytic results. The data of MD012404 (red circles) are all located between the end members of Meiha Lake in northeastern Taiwan on the I-lan Plain and sources in China. (For interpretation of the references to colour in this figure legend, the reader is referred to the web version of this article.)

Semi-quantitative calculations use the characteristic peak area of each mineral, which are summed on a percentage basis (no weightings are given). The use of different methods (peak height intensity or peak area) and different weighting factors to estimate amounts of clay minerals by previous researchers (Biscaye, 1965; Chen, 1973; Lin and Chen, 1983; Eisma et al., 1995) make it difficult to compare their results with those of the semi-quantification method. Consequently, this study (Table 2) uses only the integration of peak areas without weighting factors to estimate the “relative percentage” of major minerals, but it is not the true percentage. A  $d$ -spacing of 9.9 Å represents illite (and/or mica), 7.1 Å for chlorite and kaolinite, 3.34 Å for quartz, 3.18–3.24 Å for feldspar, 3.03 Å for calcite, and 2.89 Å for dolomite. However, because peak 7.1 Å includes the contributions of both kaolinite and chlorite, their respective percentages are dependent on the ratio of peak heights at 3.54 Å (0 0 4), a reflection of chlorite, and 3.57 Å (0 0 2) reflecting kaolinite (Biscaye, 1965). It was found that kaolinite content was minute to nearly zero in most bulk sediments, so it is not included in our mineralogical results. Use of *Peak Fit 4.2* software aided in calculating the peak area of each characteristic peak after removing  $K\alpha_2$  and subtracting background results. Mineral identification gives: quartz, feldspar, illite, chlorite, and calcite as present. Good correlation was given between carbonate-content data obtained using XRD semi-quantification with that of carbonate values obtained using traditional acid treatment (Chang et al., 2005) (Fig. 2). The total terrestrial contributions in the mineralogical data were estimated by subtracting biogenic carbonate contents (calcite and dolomite) from the sum of all peak height areas of the other minerals.

The actual content of major chemical compounds in bulk sediments was determined using wavelength-dispersive XRF (RIGAKU RIX-2000) analysis to USGS standards (see Yang et al. (1996) for analysis procedures and precision references for measured elements). The analytical major compounds include:  $\text{SiO}_2$ ,  $\text{Al}_2\text{O}_3$ ,  $\text{Fe}_2\text{O}_3$ ,  $\text{TiO}_2$ ,  $\text{CaO}$ ,  $\text{K}_2\text{O}$ ,  $\text{Na}_2\text{O}$ ,  $\text{MgO}$ ,  $\text{MnO}$ , and  $\text{P}_2\text{O}_5$ , which help to

explain different detrital sources.  $\text{Al}_2\text{O}_3$ , for example, is considered a residual compound in deposited sediments. In order to show variations in elemental ratios relative to residual elements, and subtract the dilution effect of calcium carbonate from biogenic sources, each element was normalized to Al. This approach can help identify those components that are enriched or depleted in detrital sediments.

## 5. Age and sedimentation rates

A preliminary age model of core MD012404 has been published previously (Chang et al., 2005). That age model was based on only five Accelerator Mass Spectrometry (AMS)  $^{14}\text{C}$  dates and 16 oxygen isotope age controls from a SPECMAP stack (Imbrie et al., 1984). In this study, an improved age model for the core is presented using 19 AMS  $^{14}\text{C}$  ages in the last 40,000 years, and seven oxygen isotope age control points determined from correlation between the benthic isotope curve and high resolution stack curve (Imbrie et al., 1984; Pisias et al., 1984; Martinson et al., 1987; Chang et al., 2009) (see Table 1, which includes the five  $^{14}\text{C}$  dates from Chang et al., 2009). The AMS  $^{14}\text{C}$  measurements were done by taking ~20 mg of planktic foraminifers *Globigerinoides ruber* and *Globigerinoides sacculifer* (>250  $\mu\text{m}$ ). These microfossils were then dated at the Micro Analysis Laboratory, Tandem Accelerator Mass Spectrometry Facility, University of Tokyo. All ages were adjusted for a mean Pacific reservoir age of 400 years, and then calibrated according to Fairbanks et al. (2005). Continuous time series were established by linear interpolation between each pair of calibrated  $^{14}\text{C}$  dates, with the basal age of the core identified as ~100 ka, representing the late Marine Isotope Stage 5 (MIS 5).

The preliminary age model, using oxygen isotope stages, was presented in previous studies by Chang et al. (2005, 2008, 2009) and the sedimentation rate based on these initial results shows to be high at ~50 cm/ky. Fig. 3a shows our new age model with

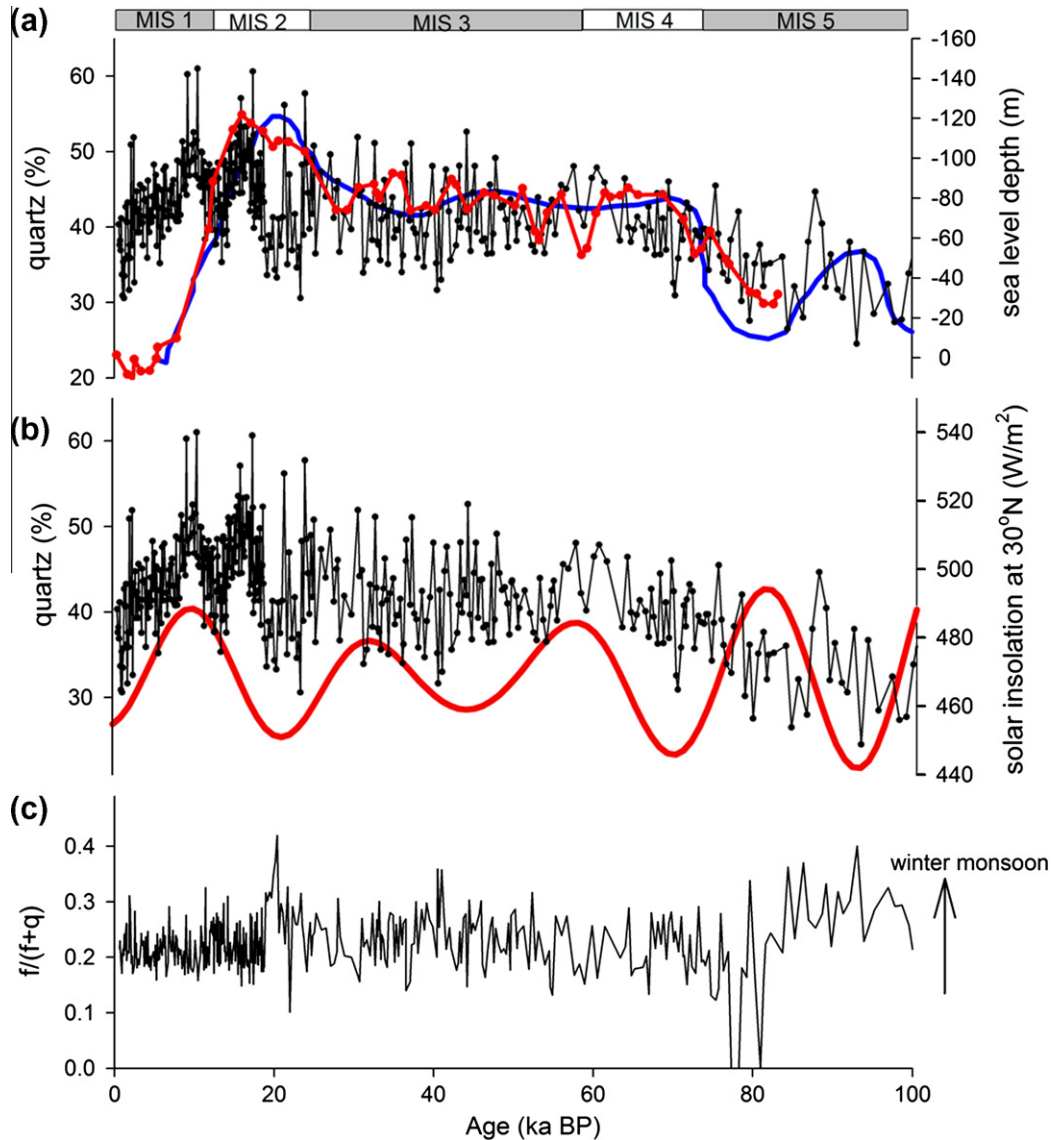


**Fig. 5.** Relationship between quartz content and: (a) sea-level depth and (b) average summer solar insolation at 30°N (June, July and August). (c) Feldspar/(feldspar + quartz) ratios. Sea-level depth is shown with a reverse coordinate axis, and represented by the red dotted line (Saito et al., 1998) and the blue continuous curve (Cutler et al., 2003) in Fig. 5a. Prior to 24 ka, the quartz content and sea-level change display very good agreement. After 24 ka, further influence from the summer solar insolation plays a further important role.  $F/(F+Q)$  ratios display anomalously high at 20 ka and 40 ka, and extremely low during 80 ka varying inversely to the summer solar insolation. (For interpretation of the references to colour in this figure legend, the reader is referred to the web version of this article.)

additional  $^{14}\text{C}$  dates. This model has high resolution of  $\sim 0.1$  ky after 20 ka. Note that relatively low sedimentation rates existed before  $\sim 80$  ka with rates gradually increasing after  $\sim 60$  ka. In fact, sedimentation rates are relatively high at:  $\sim 35$  ka,  $\sim 24$  ka,  $\sim 18$  ka, and  $\sim 14$  ka (Fig. 3a).

## 6. Results

### 6.1. Detrital sources

Our analytic results of calcite (and rare dolomite) content by XRD (Fig. 2) agree well with the acid treatment results of Chang et al. (2005), except for calcite amounts higher than 25%. This gives credibility to the semi-quantitative XRD method used in this study. In order to better understand terrestrial-sediment sources, calculations to determine the percentage contribution of major detrital minerals are based on the presence of quartz,

feldspar, illite and chlorite without calcite and dolomite content. Fig. 3b presents the relative contributions of these major detrital minerals after 100 ka. The figure shows quartz content varying inversely with illite and chlorite, whilst feldspar is generally relatively stable except for two large variations during 20 ka and 80 ka. Much can be inferred about these differences in content trends. For example, such trends suggest quartz being carried from a different source relative to illite and chlorite or they could represent grain size variation from source distance changes in the reaches of the Yangtze River due to sea-level variations. To probe source regions, we compare the results of relative mineral contents from China with those from Taiwan (Table 2) and plot the data in a ternary diagram (Fig. 4). For north China, we have mineral data from Inner Mongolia and the Nihawan Basin (at high latitudes). Core data from a dried saline lake in Inner Mongolia shows lakeshore to aeolian sand layers in its upper section, and lacustrine mud in its lower section. For the lakeshore and aeolian

sand, sediments are rich in quartz and feldspar. For lake facies, sediments are rich in clay fractions (Chen et al., 2010). The sediments of the Nihawan Basin near the Löss Plateau in north China are also rich in quartz and feldspar. On the other hand, we analyzed mineral data from three lakes in Taiwan: Meiha Lake on the I-lan Plain of northeast Taiwan, Liyutan Lake in central Taiwan, and Tung-Yuan Pond in southern Taiwan, and found the clay fractions in the sediments from northeast Taiwan are higher than those from Inner Mongolia, the Yellow River and Yangtze River (Yang et al., 2004) (Fig. 4). As to quantitative methods for major minerals, Yang et al. (2004) used microscopy to count the percentage of minerals in coarse grains, and XRD to count the clay fractions; therefore, we cannot directly compare their data with ours. We can transfer Yellow River (Y1) data to that of the Nihawan Basin because the two places are similar in geological environment. Fig. 4 shows transferred data of the Yellow River (Y1) and Yangtze River (Y2) to the concentrated data of our analytical results. Sediments from MD012404 locate between the two end members of the Yangtze River and Meiha Lake (M). This proves that sediments at MD012404 are not related to those of lakes Liyutan (L) and Tung-Yuan (T) in central and southern Taiwan. In addition, we can infer that detrital sediments along northeastern Taiwan shelves are similar to those in Meiha Lake (M).

According Yang et al.'s data (2004), the feldspar ratio of the Yellow River is higher than that of the Yangtze River (Table 2). We propose that the deposited sediments from China contain more quartz and feldspar; however, feldspar decomposes to kaolinite due to chemical weathering after long riverain and oceanic transportations. This leads to less feldspar content in oceans and lakes; however, feldspar content could be rich if it arrived via aeolian transportation (Chen et al., 2010). The ratio of feldspar/(feldspar + quartz) is not constant in core MD012404 (Fig. 5c) because it is influenced by varying sources. The ratio of feldspar/(feldspar + quartz) is high in northern China, particularly in aeolian sands and the Löss Plateau (Table 2). We assume that some feldspar in core MD012404 is derived via aeolian transportation from northern China. The average ratio of feldspar/(feldspar + quartz) is about 0.2 in core MD012404. This is higher than for Taiwan lakes ( $\leq 0.04$ ). Interestingly, the feldspar/(feldspar + quartz) ratio in core MD012404, dramatically increases at  $\sim 20$  ka and 40 ka, and swiftly decreases to near zero during 80 ka (Fig. 5c). Fig. 5b and c show an apparent opposite relationships between the summer solar insolation and the ratio of feldspar/(feldspar + quartz). We infer that the ratio is indicative of feldspar arriving on aeolian transportation, which was strengthened by the winter monsoon. During the LGM, when ice covered north Asia at 22 ka, aeolian sources were

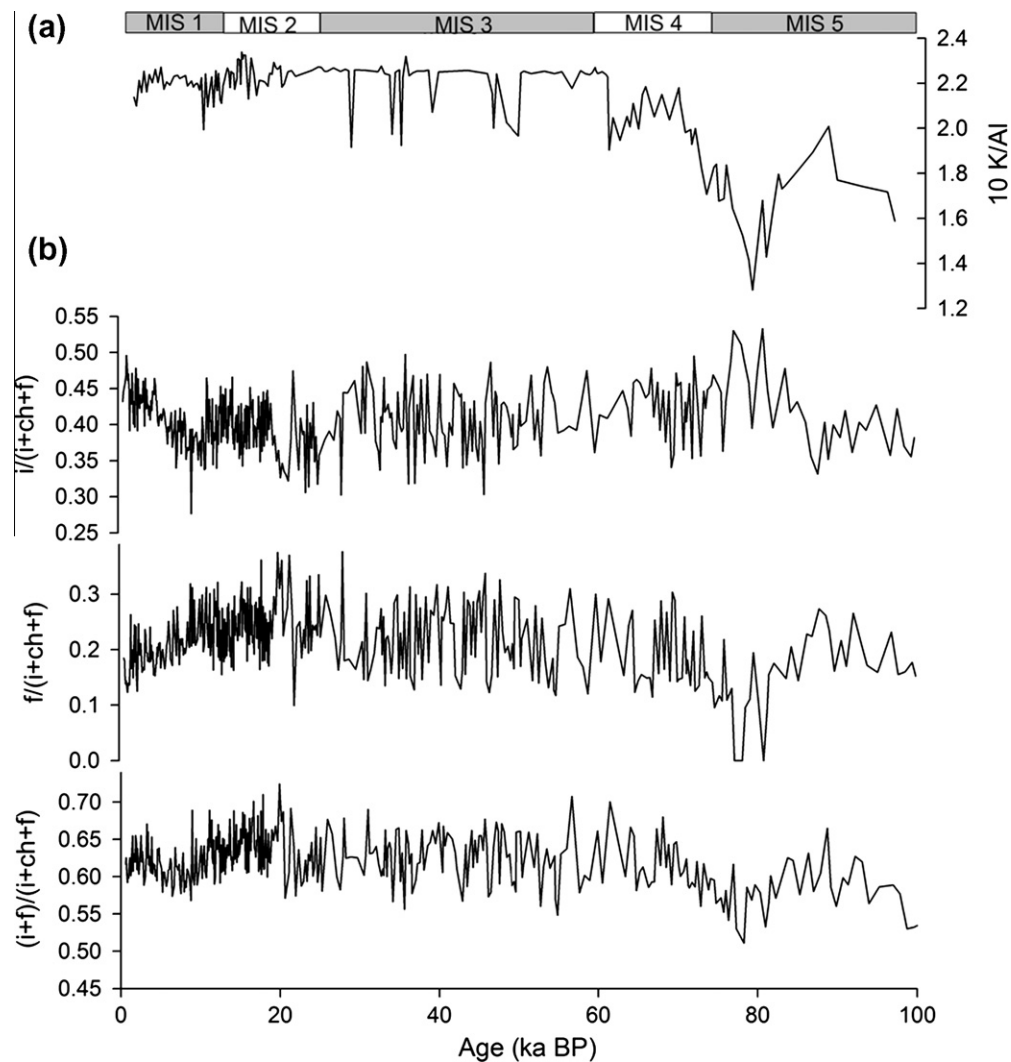


**Fig. 6.** The K/Al ratio gives the contributions of illite and K-feldspar in this core. It represents the sum of illite and feldspar (bearing K) in proportion Al-bearing minerals, which include illite, chlorite and feldspar. (a) The ratio of 10 K/Al by XRF with relation to (b) illite/(illite + chlorite + feldspar), feldspar/(illite + chlorite + feldspar), and (illite + feldspar)/(illite + chlorite + feldspar).

reduced causing the feldspar/(feldspar + quartz) ratio to be low. When the ice started to melt at 20 ka, the aeolian signal abruptly rose (Fig. 5c). These distinct anomalous signals of feldspar/(feldspar + quartz) coincide with the minima and maxima of solar insolation. Throughout the wider North Pacific Ocean, many reports have pointed to aeolian transport from north Asia at 38–40°N due to strong winter monsoons. Aeolian dust prevailed toward southern and eastern regions during glacial periods. Especially, the Japan (Iriino and Tada, 2002; Nagashima et al., 2007) and South China Seas (Liu et al., 2003), which received a great deal of aeolian dust when strong winter winds occurred during glacial periods. Nagashima et al. (2007) proved good correlations between aeolian-dust transport and solar insolation with aeolian dust also being extremely high around 20 ka and 40 ka, and extremely low around 80 ka. Signal variations for aeolian transport to the central OT are not likely to be as pronounced as those for Japan, and are probably only evident for extreme climate variations.

Comparing sedimentation-rate results (Fig. 3a) with variations in minerals (Fig. 3b), quartz content tracks sedimentation rates positively and closely prior to 16 ka, but presents an inverse relationship after 16 ka. After 16 ka, chlorite and illite content vary positively with sedimentary rates. These results indicate that prior to 16 ka sediment was sourced primarily from the Yangtze River (i.e. in phase variations in quartz content and sedimentary rates); however, after this date, synchronous trends in chlorite and illite with sedimentary rates suggest another source affecting the OT. We propose more KC water flowing into the OT after 16 ka, bringing with it more illite and chlorite from eastern Taiwan. It is interesting to note quartz decreased by about 15% during 24–19 ka (Fig. 3b). At 20 ka, opposite variations in quartz and feldspar content indicate reduced inflow from the Yangtze River during the

LGM and aeolian transport to the central OT from inland China being dominant.

## 6.2. Geochemistry of the major elements

Al is a weathering resistant element that can be used to understand long-term variations of bulk sediments under chemical weathering. The content of each compound is divided by Al content with these ratios representing the relative amounts of each to amounts of clay and feldspar, excluding the dilution of calcite and quartz contents. Our results for Na/Al and P/Al show similar variations to those of carbonates. This is indicative of Na and P being supplied by pore water in the sediment, which can be highly affected by porous biogenic materials. We, therefore, use the Na/P ratio to avoid any influence from fluid content. XRF data for the results of K/Al, Ti/Al, and Na/P show some interesting findings (Figs. 6a and 7):

- K/Al ratio shows its lowest value at ~78.3 ka after which time an apparent increasing trend occurs until ~64 ka. Post 64 ka, the 10 K/Al ratios fluctuate narrowly between 2 and 2.3 through to MIS 3 to 1. Considering mineral contributions, illite and K-feldspar are the major sources of K. In our core, most XRD peaks of feldspar are close to K-feldspar. To identify why the K/Al ratio decreased during 80 ka, we plot illite/(illite + chlorite + feldspar) and feldspar/(illite + chlorite + feldspar) variations in Fig. 6b. Variation in the K/Al ratios are congruent with (illite + feldspar)/(illite + chlorite + feldspar) variations. This indicates the most likely reason for a decreasing K/Al ratio is a decline in feldspar during 80 ka. This K/Al ratio supports the previously mentioned anomalous decrease in feldspar during 80 ka (Fig. 3b).

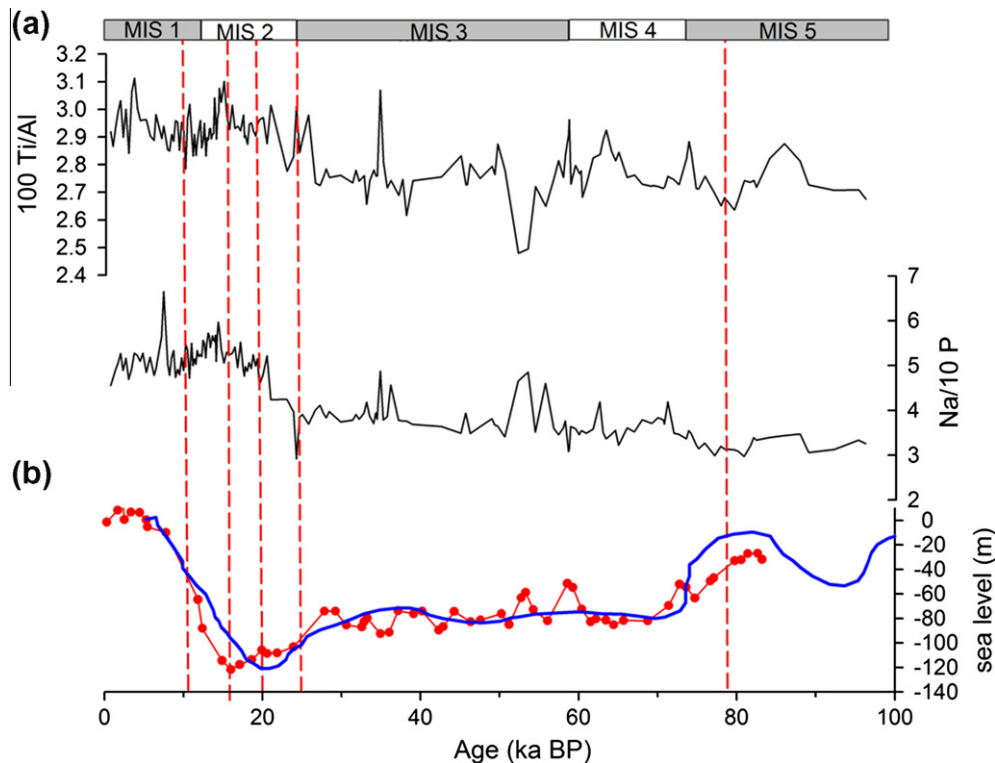


**Fig. 7.** (a) The elemental ratios of 100Ti/Al, Na/10P by XRF with relation to (b) sea-level change according to digitized data from Saito et al. (1998) and Cutler et al. (2003). The red dotted line tracks the post-glacial transgression of the ECS area from Saito et al. (1998). The blue continuous curve refers to Cutler et al. (2003). The dashed-red lines represent the time boundaries at: 78.3 ka, 24 ka, 19 ka, 16 ka, and 10 ka. (For interpretation of the references to colour in this figure legend, the reader is referred to the web version of this article.)

- The Ti/Al ratio exhibits a relatively high value after ~26 ka, and reaches a confirmed high after 20 ka. During 26–100 ka, the average of the 100Ti/Al ratios was about 2.76, but it rose to 2.93 after 26 ka (Table 3, Fig. 7a). Before 20 ka, an extremely high ratio appeared at 34.7 ka. Comparing Ti/Al ratios in Table 3, Ti/Al ratio is lower in continental crust and felsic rocks ( $\leq 2.89$ ), but higher in mafic rocks ( $\sim 5.33$ ). In our core, the Ti/Al ratio is between that of upper and lower continental crusts. Indeed, sediments show an increasing Ti/Al ratio after 26 ka. This phenomenon implies sediment transport from eastern Taiwan via the KC perhaps entering the OT after this time. Eastern Taiwan is mainly composed of oceanic crust with rich mafic rocks. After 16 ka, the Ti/Al displayed an anomalous increase.
- The Na/P ratio reveals changes in salinity with low salinity sea water prevalent before about 20 ka, increasing until the present. This is a similar trend to variations in the Ti/Al ratio, but the onset time for its increase is later than that of Ti/Al.

The above elemental variations indicate that Ti/Al and K/Al represent detrital sources, whilst Na and P are mainly dependent on the water systems. Chen et al. (1995a) point to the KTW having the highest salinity of all KC water, so the Na/P ratio may reflect intrusion of the KTW into the OT.

## 7. Discussion

In this study, mineralogical and geochemical results obtained from MD012404 show variations in the supply of detrital sediments over the last ~100 ka in the central OT. Results indicate that the Yangtze River was the main source of terrestrial sediments from 100 to 16 ka, except for 24–19 ka when fluvial sources decreased and aeolian supply increased. After 16 ka, variations in illite and chlorite indicate that terrestrial sediments carried on the Kuroshio from eastern Taiwan gradually replaced those from the ECS (Fig. 3a and b). Observed quartz variations of Fig. 5a show quartz content matching sea-level variation during MIS 3, 4 and 5; these results fit well the sea-level results of Saito et al. (1998). In Fig. 5a, higher sea-levels (~–40 m) during MIS 5 resulted in a quartz content of less than 35%; however, lower sea-levels (~–80 m) during MIS 3 led to quartz content being higher at about 45%. This relationship between falling sea-levels and increasing quartz content is evident until 24 ka. Accordingly, we can assume that the supply of quartz is mainly from the Yangtze River and the ESC basin before 24 ka. As the sea-level dropped, the reach of the Yangtze River was closer to the central OT, improving the supply of coarser sediments. Conversely, during MIS 5, sea-levels were higher and Yangtze River supply was farther away from the coring site, leading to finer transported sediments and rich clay in the core.

However, after 24 ka, there is a decoupling between quartz content and sea-level changes (Fig. 5a). When sea-levels were at their lowest (about –120 m) during the LGM, quartz content abruptly decreased to its lower limit. It swiftly increased again, however, around 19 ka. During the LGM, the Yangtze River mouth was situated at the shelf edge close to the central OT (Ujiié et al., 2001). When summer solar insolation was very low during the LGM (Fig. 5b), water supply from the upper Yangtze died away due to freezing conditions on the Tibetan Plateau from 24 to 19 ka. Contemporaneously, aeolian transport exhibits great variation between 22 and 20 ka. In Section 6, we discussed the inverse relationship between summer solar insolation and feldspar/(feldspar + quartz) ratios. After 19 ka, quartz supply increased swiftly and large amounts of sediment arrived until 16 ka (Fig. 3b). According to previous research, sedimentation rates did increase from about 19 ka (Fig. 3a) (Xu and Oda, 1999; Xiang et al., 2007).

The notion is supported by faunal evidence (Xu and Oda, 1999) and organic matter composition (Ujiié et al., 2001). After this period of sudden increase, quartz content again declined to its lower limits and established its previous trend of varying with sea-levels until 13 ka (Fig. 5a). Interestingly, quartz content also peaked in 10 ka under the influence of high summer insolation (Fig. 5b). This suggests terrestrial-river input and/or the KC strengthening due to reinforcement of the summer monsoon. In the early Holocene, climatic conditions led to maximum summer monsoon conditions, causing overall high temperatures and humidity in East Asia and the Yangtze River (Yi and Saito, 2004). This result has also been recorded in ice-core records from the Tibetan Plateau (Thompson et al., 1997).

The geochemical results given in Section 6.2 suggest a change in terrestrial sediment supply from the ECS to the eastern shelves of Taiwan due to the presence of higher Ti/Al ratios after 26 ka. In addition, high Na/P ratios also reflect the intrusion of KTW. Ti is often concentrated in basic rocks and oceanic crusts (Rudnick and Fountain, 1995; Klein, 2003; Rudnick and Gao, 2003). Geologically, western Taiwan is composed of continental crust, and eastern Taiwan is composed of oceanic crust. Increased Ti/Al ratios imply sediment sources from eastern Taiwan. In the southern OT, a series of turbidites occurred in core OPD1202 during 60–30 ka (Huang et al., 2005); these are indicative of mass-wasting events during this period. Kao et al. (2006) suggest a tectonic event during this period that might have caused a topographic barrier to be broken and the Yonaguni Depression to be formed. In core ODP1202, clay sediments were deposited after 28 ka (Diekmann et al., 2008). In addition, volcanic activity in Japan (Machida, 2002) indicates two eruptions (Aira (Aira-Tn) Volcano, 29–26 ka; Kikai (K-Ah) Volcano at 7.3 ka) in Kyushu that would have led to transported volcanic ash to this area. The Aira volcanic explosion was violent and long. These events in the southern OT and southern Japan could indicate continuous tectonic opening in the OT which potentially led to Ti/Al ratios increasing after 26 ka. We did not, however, find any Aira-ash geochemical signals from 29 to 26 ka, though Kikai-ash signals exist at 7.3 ka in the form of an anomalous increase in Si/Al ratios, and the presence of volcanic ash in the core (Chang et al., 2008). Given the above analysis, an increased Ti/Al ratio implies intrusion of the KC into the OT carrying with it sediments from eastern Taiwan. This could reflect a tectonic opening in the southern OT during ~26 ka. In addition, previous research of diatom evidence in core MD012404 (Chang et al., 2008) supports warm-tropical species intruding into the OT at 29–25 ka; these gradually increase after about 20 ka. These results coincide with our Ti/Al ratio increases (Fig. 7a). Therefore, it implies that more KC was able to enter the OT freely after about 20 ka.

Moreover, our Na/P ratio also suggests that low salinity water prevailed prior to 20 ka, and the salinity has increased since that time.

## 8. Conclusions

This study uses geochemical and mineralogical data derived from the sedimentary record of IMAGES Core MD012404 to infer sea-level changes and the influence of the Asian monsoon based on the terrestrial sediments found in the core. The sediment record is examined for the past 100 ka. Terrestrial sediments of IMAGES Core MD012404 are sourced mainly from the Yangtze River and Kuroshio Current. Accordingly, we can infer that sediments sourced from the Yangtze River reflect sea-level changes before 24 ka. In addition, there is some evidence of other sediments entering the Okinawa Trough, perhaps from eastern Taiwan, at around 26 ka, according to higher Ti/Al ratios. There is also evidence of declining fluvial sediments from the Yangtze during the LGM

period. However, at this time, the Yangtze Estuary was still close to the central Okinawa Trough so that when the climate began warming after 19–20 ka, abrupt increases in Na/P ratios and in the amount of quartz in the core are apparent. From these two findings, we speculate that more KTW may have intruded into the Okinawa Trough and more water may have flowed into the ECS from the Yangtze River since then. The feldspar anomalies may imply that the eolian sources changed, caused by the varying strengths of the East Asian winter monsoon.

## Acknowledgements

This study was supported by National Taiwan Ocean University and Grants: NSC95-2611-M-019-013 and NSC 97-2116-M-019-004 from the National Science Council of Taiwan. We are grateful to Mr. Mao-Hsiang Chiu and Pai-Sen Yu for their computer work. We acknowledge the crew and scientists on board the RV Marion Dufrenoy for retrieving IMAGES core MD012404. In addition, the XRD and XRF experiments were carried out at National Taiwan University. We deeply appreciate Dr. Chi-Yu Lee for providing support for the conventional XRF.

## References

- Andres, M., Wimbush, M., Park, J.H., Chang, K.I., Lim, B.H., Watts, D.R., Ichikawa, H., Teague, W.J., 2008. Observations of Kuroshio flow variations in the East China Sea. *Journal of Geophysical Research* 113, C05013. doi:10.1029/2007JC004200.
- Aoki, S., Oinuma, K., 1974. Clay mineral compositions in recent marine sediments around Nansei-Syoto Islands, south of Kyusyu, Japan. *The Journal of the Geological Society of Japan* 80, 57–63.
- Bassinot, F.C., Baltzer, A., Chen, M.T., DeDeckker, P., Khuht, W., Levitan, M., Nurnberg, D., Oba, T., Prentice, M., Sarnthein, M., Situmorang, M., Tiedemann, R., Holbourn, A., Kiefer, T., Pflaumann, U., Rothe, S., 2002. Scientific Report of the WEPAMA Cruise, MD122/IMAGES VII.
- Beardsley, R.C., Limeburner, R., Yu, H., Cannon, G.A., 1985. Discharge of the Changjiang (Yangtze River) into the East China Sea. *Continental Shelf Research* 4 (1–2), 57–76.
- Biscaye, P.E., 1965. Mineralogy and sedimentation of recent deep-sea clay in the Atlantic Ocean and adjacent seas and oceans. *Geological Society of America Bulletin* 76, 803–832.
- Chang, Y.P., Wu, S.M., Wei, K.Y., Murayama, M., Kawahata, H., Chen, M.T., 2005. Foraminiferal oxygen isotope stratigraphy and high-resolution organic carbon, carbonate records from the Okinawa Trough (IMAGES MD012404 and ODP Site 1202). *Terrestrial Atmospheric and Oceanic Sciences* 16 (1), 57–73.
- Chang, Y.P., Wang, W.L., Yokoyama, Y., Matsuzaki, H., Kawahata, H., Chen, M.T., 2008. Millennial-scale planktic foraminifer faunal variability in the East China Sea during the past 40,000 years (IMAGES MD012404 from the Okinawa Trough). *Terrestrial Atmospheric and Oceanic Sciences* 19 (4), 389–401.
- Chang, Y.P., Chen, M.T., Yokoyama, Y., Matsuzaki, H., Thompson, W.G., Kao, S.J., Kawahata, H., 2009. Monsoon hydrography and productivity changes in the East China Sea during the past 100,000 years: Okinawa Trough evidence (MD012404). *Paleoceanography* 24, PA3208. doi:10.1029/2007PA001577.
- Chen, P.Y., 1973. Clay minerals distribution in the sea-bottom sediments neighbouring Taiwan Island and northern South China Sea. *Acta Oceanographica Taiwanica* 3, 25–64.
- Chen, C.T.A., 1996. The Kuroshio intermediate water is the major source of nutrients on the East China Sea continental shelf. *Oceanologica Acta* 19, 523–527.
- Chen, C.T.A., Wang, S.L., 1998. Influence of intermediate water in western Okinawa Trough by the outflow from the South China Sea. *Journal of Geophysical Research* 103 (C6), 12683–12688.
- Chen, J.Y., Shen, H.T., Yun, C.X., 1988. Process of Dynamics and Geomorphology of the Changjiang Estuary. Shanghai Science and Technology Press, Shanghai.
- Chen, C.T.A., Ruo, R., Pai, S.C., Liu, C.T., Wang, G.T.F., 1995a. Exchange of water masses between the East China Sea and the Kuroshio off northeastern Taiwan. *Continental Shelf Research* 15 (1), 19–39.
- Chen, C.T.A., Liu, C.T., Pai, S.C., 1995b. Variations in oxygen, nutrient and carbonate fluxes of the Kuroshio Current. *La Mer* 33, 161–176.
- Chen, Z., Li, J., Shen, H., Zhanghua, W., 2001. Yangtze River of China: historical analysis of discharge variability and sediment flux. *Geomorphology* 41 (2–3), 77–91.
- Chen, Z., Saito, Y., Kanai, Y., Wei, T., Li, L., Yao, H., Wang, Z., 2004. Low concentration of heavy metals in the Yangtze estuarine sediments, China: a diluting setting. *Estuarine, Coastal and Shelf Science* 60 (1), 91–100.
- Chen, H.F., Song, S.R., Lee, T.Q., Löwemark, L., Chi, Z.Q., Wang, Y., Hong, E., 2010. A multiproxy lake record from Inner Mongolia displays a late Holocene teleconnection between central Asian and North Atlantic climate. *Quaternary International* 227, 170–183.
- Cutler, K.B., Edwards, R.L., Taylor, F.W., Cheng, H., Adkins, J., Gallup, C.D., Cutler, P.M., Burr, G.S., Bloom, A.L., 2003. Rapid sea-level fall and deep-ocean temperature change since the last interglacial period. *Earth and Planetary Science Letters* 206, 253–271.
- DeMaster, D.J., McKee, B.A., Nittrouer, C.A., Qian, J., Cheng, G., 1985. Rates of sediment accumulation and particle reworking based on radiochemical measurements from continental shelf deposits in the East China Sea. *Continental Shelf Research* 4 (1–2), 143–158.
- Diekmann, B., Hofmann, J., Henrich, R., Fütterer, D.K., Röhl, U., Wei, K.Y., 2008. Detrital sediment supply in the southern Okinawa Trough and its relation to sea-level and Kuroshio dynamics during the late Quaternary. *Marine Geology* 255, 83–95.
- Dorsey, R.J., Buchovecky, E.C., Lundberg, N., 1988. Clay mineralogy of Pliocene–Pleistocene mudstones, eastern Taiwan: combined effects of burial diagenesis and provenance unroofing. *Geology* 16, 944–947.
- Eisma, D., Ji, Z., Chen, S., Chen, M., van der Gaast, S.J., 1995. Clay mineral composition of recent sediments along the China coast in the Yellow Sea and the East China Sea. NIOZ-Rapport 1995-4. Nederlands Instituut voor Onderzoek der Zee.
- Fairbanks, R.G., Mortlock, R.A., Chiu, T.C., Cao, L., Kaplan, A., Guilderson, T.P., Fairbanks, T.W., Bloom, A.L., Grootes, P.M., Nadeau, M.J., 2005. Radiocarbon calibration curve spanning 0 to 50,000 years BP based on paired  $^{230}\text{Th}/^{234}\text{U}$  and  $^{14}\text{C}$  dates on pristine corals. *Quaternary Science Reviews* 24 (16–17), 1781–1796.
- Hsin, Y.C., Wu, C.R., Shaw, P.T., 2008. Spatial and temporal variations of the Kuroshio east of Taiwan, 1982–2005: a numerical study. *Journal of Geophysical Research* 113, C04002. doi:10.1029/2007JC004485.
- Huang, C.Y., Chiu, Y.L., Zhao, M.X., 2005. Core description and a preliminary sedimentology study of site 1202D, Leg 195, in the southern Okinawa Trough. *Terrestrial Atmospheric and Oceanic Sciences* 16, 19–44.
- Ijiri, A., Wang, L., Oba, T., Kawahata, H., Huang, C.Y., 2005. Paleoenvironmental changes in the northern area of the East China Sea during the past 42,000 years. *Palaeogeography Palaeoclimatology Palaeoecology* 219, 239–261.
- Imbrie, J., Hays, J.D., Matinson, D.G., McIntyre, A., Mix, A.C., Morley, J.J., Pisias, N.G., Prell, W.L., Shackleton, N.J., 1984. The Orbital Theory of Pleistocene Climate: Support from a Revised Chronology of the Marine  $\delta^{18}\text{O}$  Record. D. Reidel Publishing Company, pp. 269–305.
- Irino, T., Tada, R., 2002. High-resolution reconstruction of variation in aeolian dust (Kosa) deposition at ODP site 797, the Japan Sea, during the last 200 ka. *Global and Planetary Change* 35, 143–156.
- Jian, Z., Wang, P., Saito, Y., Wang, J., Pflaumann, U., Oba, T., Cheng, X., 2000. Holocene variability of the Kuroshio Current in the Okinawa Trough, northwestern Pacific Ocean. *Earth and Planetary Science Letters* 184, 305–319.
- Kao, S.J., Roberts, A.P., Hsu, S.C., Chang, Y.P., Lyons, W.B., Chen, M.T., 2006. Monsoon forcing, hydrodynamics of the Kuroshio Current, and tectonic effects on sedimentary carbon and sulfur cycling in the Okinawa Trough since 90 ka. *Geophysical Research Letters* 33, L05610. doi:10.1029/2005GL025154.
- Klein, E.M., 2003. Geochemistry of the igneous oceanic crust. In: *Rundnick, R.L. (Ed.), Treatise on Geochemistry*, vol. 3. Elsevier, pp. 433–463.
- Lee, H.J., Chao, S.Y., 2003. A climatological description of circulation in and around the East China Sea. *Deep-Sea Research, Part II: Topical Studies in Oceanography* 50 (6–7), 1065–1084.
- Lin, F.J., Chen, J.C., 1983. Textural and mineralogical studies of sediments from the southern Okinawa Trough. *Acta Oceanographica Taiwanica* 14, 26–41.
- Liu, Z., Saito, Y., Li, T., Berne, S., Cheng, Z., Li, P., Li, Z., Guichard, F., Floch, G., 1999. Millennial-scale paleoceanography in the Okinawa Trough during the Late Quaternary period. *Chinese Science Bulletin* 44, 1705–1709.
- Liu, Z., Trentesaux, A., Clemens, S.C., Colin, C., Wang, P., Huang, B., Boulay, S., 2003. Clay mineral assemblages in the northern South China Sea: implications for East Asian monsoon evolution over the past 2 million years. *Marine Geology* 201, 133–146.
- Liu, J.P., Xu, K.H., Li, A.C., Milliman, J.D., Velozzi, D.M., Xiao, S.B., Yang, Z.S., 2006. Flux and fate of Yangtze River sediment delivered to the East China Sea. *Geomorphology*. doi:10.1016/j.geomorph.2006.03.023.
- Machida, H., 2002. Volcanoes and tephra in the Japan area. *Global Environmental Research* 6, 19–28.
- Matinson, D.G., Pisias, N.G., Hays, J.D., Imbrie, J., Moore Jr., T.C., Shackleton, N.J., 1987. Age dating and the orbital theory of the ice ages: development of a high-resolution 0 to 300,000-year chronostratigraphy. *Quaternary Research* 27, 1–29.
- McKee, B.A., Nittrouer, C.A., DeMaster, D.J., 1983. Concepts of sediment deposition and accumulation applied to the continental shelf near the mouth of the Yangtze River. *Geology* 11 (11), 631–633.
- Milliman, J.D., Meade, R.H., 1983. World-wide delivery of sediment to the oceans. *Journal of Geology* 91 (1), 1–21.
- Nagashima, K., Tada, R., Matsui, H., Irino, T., Tani, A., Toyoda, S., 2007. Orbital- and millennial-scale variations in Asian dust transport path to the Japan Sea. *Palaeogeography Palaeoclimatology Palaeoecology* 247, 144–161.
- Nakamura, H., Nishina, A., Ichikawa, H., Nonaka, M., Sasaki, H., 2008. Deep countercurrent beneath the Kuroshio in the Okinawa Trough. *Journal of Geophysical Research* 113, C06030. doi:10.1029/2007JC004574.
- Oba, T., 1990. Paleoclimatographic information obtained by the isotopic measurement of individual foraminiferal specimens. In: *Proceeding of First China International Conference Oceanic Asian Marine Geology*, pp. 169–180.
- Pisias, N.G., Matinson, D.G., Moore, T.C., Shackleton Jr., N.J., Prell, W.L., Hays, J.D., Boden, G., 1984. High resolution stratigraphic correlation of benthic oxygen isotopic records spanning the last 300,000 years. *Marine Geology* 56, 119–136.

- Rudnick, R.L., Fountain, D.M., 1995. Nature and composition of the continental crust: a lower crustal perspective. *Reviews of Geophysics* 33 (3), 267–309.
- Rudnick, R.L., Gao, S., 2003. Composition of the continental crust. In: Rudnick, R.L. (Ed.), *Treatise on Geochemistry*, vol. 3. Elsevier, pp. 1–64.
- Saito, Y., Katayama, H., Ikehara, K., Kato, Y., Matsumoto, E., Oguri, K., Oda, M., Yumoto, M., 1998. Transgressive and highstand systems tracts and post-glacial transgression, the East China Sea. *Sedimentary Geology* 122, 217–232.
- Thompson, L.G., Yao, T., Davis, M.E., Henderson, K.A., Mosley-Thompson, E., Lin, P.N., Beer, J., Synal, H.A., Cole-Dai, J., Bolzan, J.F., 1997. Tropical climate instability: the last glacial cycle from a Qinghai–Tibetan ice core. *Science* 276, 1821–1825.
- Ujiié, H., Tanaka, Y., Ono, T., 1991. Late Quaternary paleoceanographic record from the middle Ryukyu Trench slope, northwest Pacific. *Marine Micropaleontology* 18, 115–128.
- Ujiié, H., Hatakeyama, Y., Gu, X., Yamamoto, S., Ishiwatari, R., Maeda, L., 2001. Upward decrease of organic C/N ratios in the Okinawa Trough cores: proxy for tracing the post-glacial retreat of the continental shore line. *Palaeogeography Palaeoclimatology Palaeoecology* 165, 129–140.
- Ujiié, Y., Ujiié, H., Taira, A., Nakamura, T., Oguri, K., 2003. Spatial and temporal variability of surface water in the Kuroshio source region, Pacific Ocean, over the past 21,000 years: evidence from planktonic foraminifera. *Marine Micropaleontology* 49, 335–364.
- Wei, K.Y., Mii, H.S., Huang, C.Y., 2005. Age model and oxygen isotope stratigraphy of site ODP 1202 in the southern Okinawa Trough, northwestern Pacific. *Terrestrial Atmospheric Oceanic Sciences* 16, 1–18.
- Xiang, R., Sun, Y., Li, T., Oppo, D.W., Chen, M., Zheng, F., 2007. Paleoenvironmental change in the middle Okinawa Trough since the last deglaciation: evidence from the sedimentation rate and planktonic foraminiferal record. *Palaeogeography Palaeoclimatology Palaeoecology* 243, 378–393.
- Xu, X., Oda, M., 1999. Surface-water evolution of the eastern China Sea during the last 36,000 years. *Marine Geology* 156, 285–304.
- Yang, F.Y., Yang, C.C., Lee, C.Y., Chung, S.L., Chen, C.H., 1996. NTUG rock standards for geochemical analysis. *Journal of the Geological Society of China* 39 (3), 307–323.
- Yang, S.Y., Jung, H.S., Dhong, I.L., Li, C.X., 2003. A review on the provenance discrimination of sediments in the Yellow Sea. *Earth-Science Reviews* 63, 93–120.
- Yang, S.Y., Jung, H.S., Li, C., 2004. Two unique weathering regimes in the Changjiang and Huanghe drainage basins: geochemical evidence from river sediments. *Sedimentary Geology* 164, 19–34.
- Yi, S., Saito, Y., 2004. Latest Pleistocene climate variation of the east Asian monsoon from pollen records of two East China regions. *Quaternary International* 121, 75–87.